Modeling and Measurement of Eddy Currents in the ETE Spherical Tokamak

G.O. Ludwig, E. Del Bosco, J.G. Ferreira

Associated Plasma Laboratory, National Space Research Institute
12227-010, São José dos Campos, SP, Brazil

e-mail contact of main author: ludwig@plasma.inpe.br

Abstract. A series of calculations and measurements have been made to evaluate the effect of eddy currents in the spherical tokamak ETE (Experimento Tokamak Esférico). Eddy currents occur in the central column of the conventional copper toroidal field magnet, around which the ohmic heating solenoid was tightly wound, and in the continuous wall of the vacuum vessel manufactured from inconel alloy. During the startup phase, the currents circulating in the central column strongly affect the performance of the ohmic heating system, while the currents flowing in the vacuum vessel introduce large error fields that must be compensated for successful plasma breakdown and must also be taken into account in the magnetic reconstruction procedure. Elaborate analytical models have been developed to represent both systems of currents. The results of these models are compared with experimental values of the ohmic solenoid impedance, with the operation of the ohmic heating system, and with the measured distribution of eddy currents in sections of the vacuum vessel.

1. Eddy currents in the central column of ETE

The central column of the toroidal field (TF) coils in ETE is formed by twelve trapezoidal cross section copper bars [1]. Figure 1 shows a poloidal cross section of ETE and a simplified cross section of the central column. The time evolution of the currents induced by the ohmic heating solenoid in each one of the trapezoidal bars is described by a driven diffusion equation, which can be solved by using a Green's function and partial eigenfunction expansion with the trapezoidal geometry of the bars approximated by annular sectors of equivalent area. The total flux associated with the eddy currents induced in the TF coil central column is

$$\Phi_{TF}(t) = \sum_{m,n=1}^{\infty} \Phi_{mn}(t), \tag{1}$$

where each mode of the induced field evolves according to an equation characterized by the time constant τ_{mn} of the mode and its "mutual inductance coefficient" M_{mn} with the solenoid:

$$\frac{d\Phi_{mn}}{dt} + \frac{\Phi_{mn}(t)}{(2-k)\tau_{mn}} = -\frac{M_{mn}}{2-k}\frac{di_{\Omega}}{dt}. \tag{2}$$

The coupling coefficient between bars is $k = (N^2 - N + 1)/N^2$, where $N = 12$ is the number of trapezoidal bars stacked in the central column, and i_{Ω} is the current in the ohmic heating system. The voltage in the ohmic heating solenoid in series with the pair of internal compensation coils (see Fig. 5) is

$$v_{\Omega}(t) = R_{\Omega}i_{\Omega}(t) + L_{\Omega}\frac{di_{\Omega}}{dt} + \frac{N_{\Omega}\ell_{eff}}{h_{\Omega}}\frac{d\Phi_{TF}}{dt}, \tag{3}$$

where R_{Ω}, L_{Ω}, N_{Ω} and h_{Ω} are the resistance, inductance, number of turns and length of the ohmic heating solenoid, respectively. The effective length ℓ_{eff} takes into account

the additional turns introduced by the internal compensation coils. Finally, the solenoid impedance is given by

$$Z_\Omega(\omega) = \frac{v_\Omega(\omega)}{i_\Omega(\omega)} = R_\Omega + i\omega L_\Omega - \frac{i\omega N_\Omega \ell_{eff}}{(2-k)h_\Omega} \sum_{m,n=1}^{\infty} \frac{i\omega M_{mn}}{i\omega + 1/[(2-k)\tau_{mn}]}. \tag{4}$$

An "exact" representation of the solenoid impedance was generated including 48 modes in the calculation ($m = 4$ and $n = 12$ correspond to the maximum azimuthal and radial wave numbers, respectively). Based on this representation, it has been found that an equivalent four modes approximation is sufficient to describe the effect of eddy currents for time intervals longer than about 10 μs. In the high frequency range the cooling holes in the TF coil bars introduce a small correction that can be easily inserted in Eq. 4. Furthermore, it is necessary to take into account the proximity effect in the solenoid, which gives an appreciable contribution in the intermediate frequency range of the ohmic heating system operation. Figure 2 shows a Bode plot of the ohmic solenoid impedance. The lines correspond to the theoretical results and the points to experimental values. The continuous lines correspond to the calculation over the entire frequency range, including the cooling holes and proximity effect contributions. The long dashed lines correspond to the low frequency approximation and the short dashed lines to the high frequency, skin effect approximation of the solenoid impedance in the presence of eddy currents in the central column. The experimental error is typically 5%, but may be larger in the low and high frequency ranges.

2. Eddy currents in the vacuum vessel of ETE

The distribution of eddy currents in the vacuum vessel is modeled using a thin shell approximation, curvilinear coordinates and the following spectral representation in Chebyshev polynomials for the contour of the vessel:

$$\begin{aligned} R(\theta) &= C_0 + C_1 \cos\theta - a\sum_{n=1}^{n_{max}} C_n[1 - T_n(\cos\theta)], \\ Z(\theta) &= E_V \sin\theta[C_1 - a\sum_{n=1}^{n_{max}} C_n U_{n-1}(\cos\theta)]. \end{aligned} \tag{5}$$

The coefficients C_0 and C_1 are determined by the geometric constraints $R(0) = R_0 + a$ and $R(\pi) = R_0 - a$, where R_0 and a are the major and minor radii of the toroidal vessel, respectively. The elongation E_V and the remaining coefficients C_n are determined by a least-squares fitting procedure. Using again a Green's function approach, the equation governing the induction of the surface current K_T on the thin shell is [2]

$$\frac{2\pi h_\zeta}{\sigma\delta} K_T(\overrightarrow{r}) = -\mu_0 \oint \frac{\partial K_T(\overrightarrow{r}')}{\partial t} G(\overrightarrow{r}, \overrightarrow{r}') d\ell(\theta') - \frac{\partial \Phi_{ext}(\overrightarrow{r})}{\partial t}, \tag{6}$$

where σ is the conductivity of inconel, δ is the (sectionally variable) thickness of the vacuum vessel wall, and the scale factor with respect to the toroidal angle ζ is $h_\zeta = |\partial \overrightarrow{r}/\partial\zeta| = R(\theta)$. The Green's function for the axisymmetric Ampère's law is

$$G(\overrightarrow{r}, \overrightarrow{r}') = \frac{1}{2\pi} \int \frac{\pi h_\zeta h_{\zeta'} \cos(\zeta - \zeta')}{|\overrightarrow{r} - \overrightarrow{r}'|} d\zeta', \tag{7}$$

and Φ_{ext} is the flux of the external sources. The equation for K_T has local terms depending on the shell resistivity and non-local terms depending on mutual inductance effects between diverse regions of the surface current distribution. It can be solved using a truncated Fourier series expansion for the surface current given by

$$K_T(\theta, t) = \frac{1}{2\pi h_\theta(\theta)} \left(I_T(t) + \sum_{n=1}^{\ell} I_n(t) \cos n\theta \right), \tag{8}$$

where $h_\theta = |\partial \overrightarrow{r}/\partial\theta|$. The total toroidal current flowing in the vacuum vessel is I_T. This current and the coefficients I_n satisfy a set of $\ell + 1$ equations of the form $(m = 0, 1 \ldots \ell)$

$$R_{0m}I_T(t) + L_{0m}\frac{\partial I_T}{\partial t} + \sum_{n=1}^{\ell}\left(R_{nm}I_n(t) + L_{nm}\frac{\partial I_n}{\partial t}\right) = -\sum_k L_{km}\frac{\partial I_k}{\partial t}, \qquad (9)$$

where R_{nm} and L_{nm} are resistance and mutual inductance coefficients defined by:

$$\begin{aligned}
R_{nm} &= \frac{1}{2\pi\sigma\delta}\int \frac{h_\zeta(\theta)}{h_\theta(\theta)}\cos n\theta \cos m\theta\, d\theta, \\
L_{nm} &= \frac{\mu_0}{4\pi^2}\int\left(\int G(\theta,\theta')\cos n\theta'\, d\theta'\right)\cos m\theta\, d\theta,
\end{aligned} \qquad (10)$$

and $L_{km} = \mu_0(2\pi)^{-1}\int[G_k(\theta) + G_k(-\theta)]\cos m\theta\, d\theta$ are the mutual inductance coefficients between the induced current distribution and the k pairs of external coils, which are placed symmetrically with respect to the equatorial plane and connected in series. Satisfactory results are obtained including the fundamental mode and only three harmonics ($\ell = 3$) in the calculations. The evolution with time of the eddy currents in the vessel is obtained taking into account all the coupling effects between the vessel, external coils, and eddy currents in the central column. The currents in the capacitor banks and external coils are calculated self-consistently with the eddy currents. Figure 3 shows the calculated (continuous line) and experimental values (points) of the currents in the ohmic heating solenoid and vacuum vessel for a typical test shot.

Figure 4 shows the distribution of eddy currents in sections of the vacuum vessel. The measurements (points) were taken by the insertion of a long Rogowski coil through the access ports of the vessel, as indicated in Fig. 5, plus using the Rogowski coil permanently installed outside the vacuum vessel. These measurements are subject to large errors due to stray fields and misalignment. Nevertheless, there is good agreement with the calculated distribution, particularly of the times of current inversion. In the outer, weakly coupled region (outer section 1 through flanges 0 and 1 - thick wall) the vessel response is similar to a current transformer, while the response of the inner, strongly coupled region (inner section 6 between upper and lower flanges 5 - thin wall) is similar to a voltage transformer.

The calculated current distributions will be used in future work both to model the eddy current effects in zero-dimensional simulations of the plasma discharge in the early phase, and to eliminate error-fields in the magnetic reconstruction of the plasma equilibrium.

References

[1] LUDWIG, G.O., et al. "Spherical tokamak development in Brazil". Braz. J. Phys. **33**, 848-859 (2003).

[2] LUDWIG, G.O. "Calculation of eddy currents in the ETE spherical torus". In Plasma Physics: Proceedings of the 11th International Congress on Plasma Physics, Sydney, Australia, 2002, edited by I.S. Falconer, R.L. Dewar, and J. Khachan (AIP Conf. Proc. **669**, 2003), pp. 573-576.
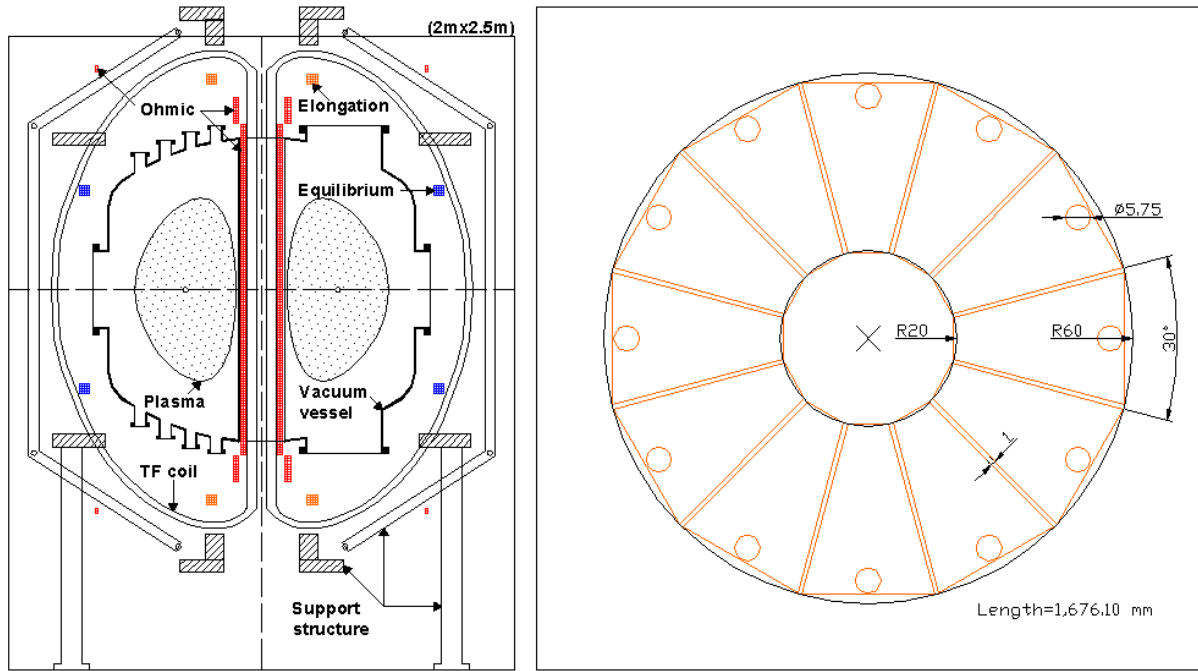
Figure 1: *Simplified cross sections of ETE and of the toroidal field coil central column.*
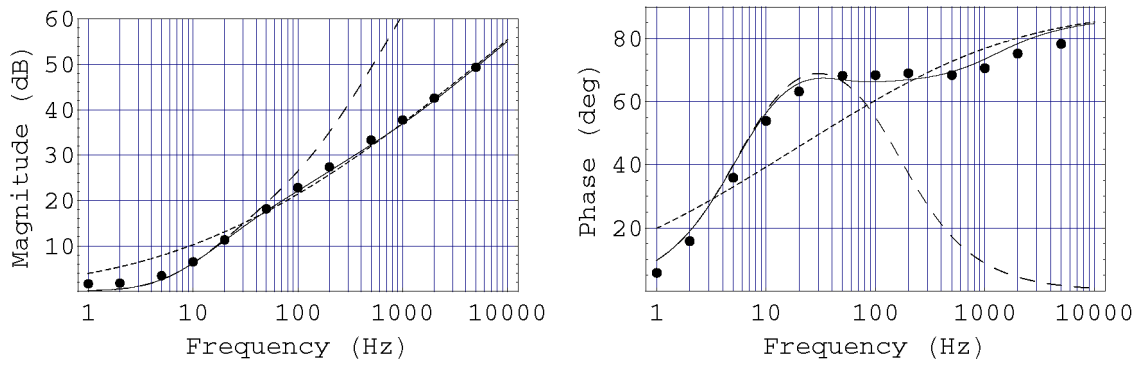

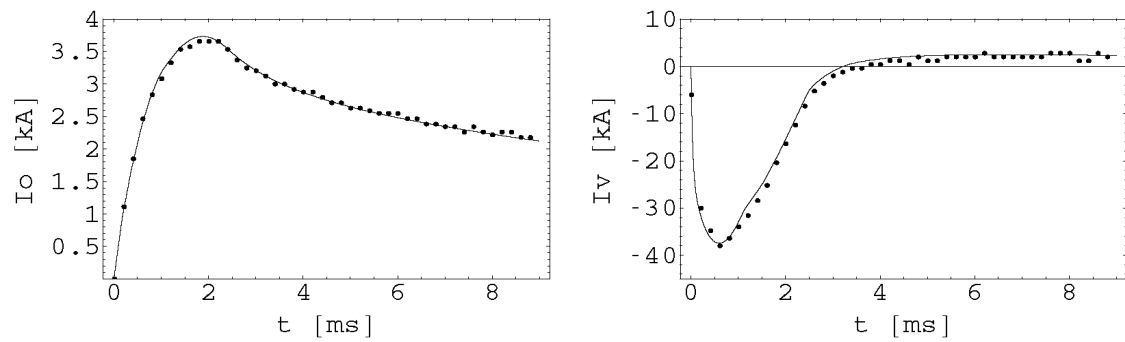Figure 2: *Amplitude and phase of the ohmic solenoid impedance.*

Figure 3: *Current in the ohmic heating system and total eddy current in the vacuum vessel.*
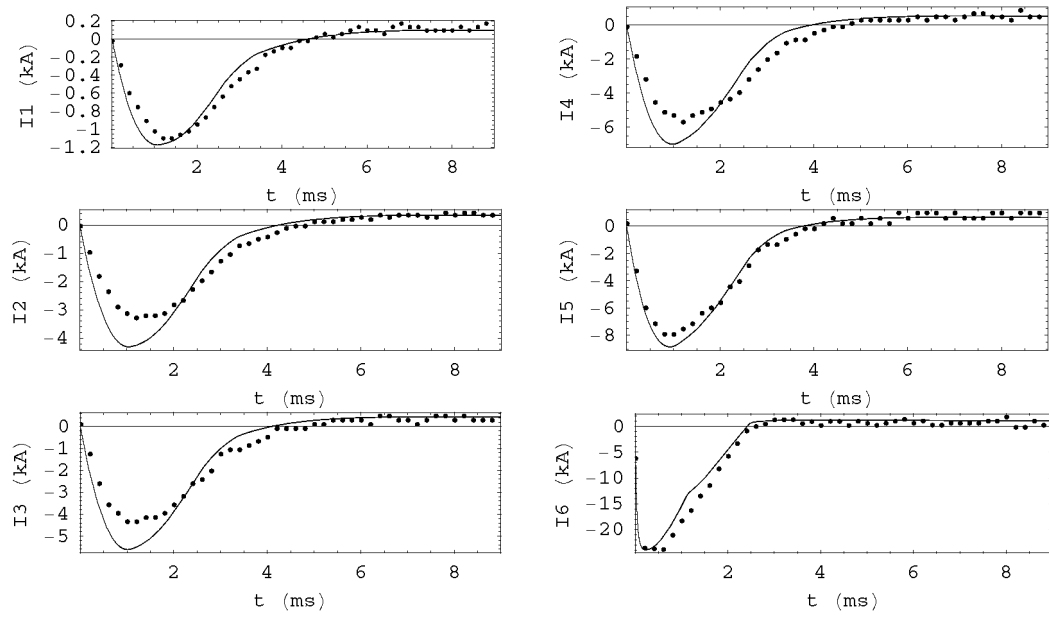
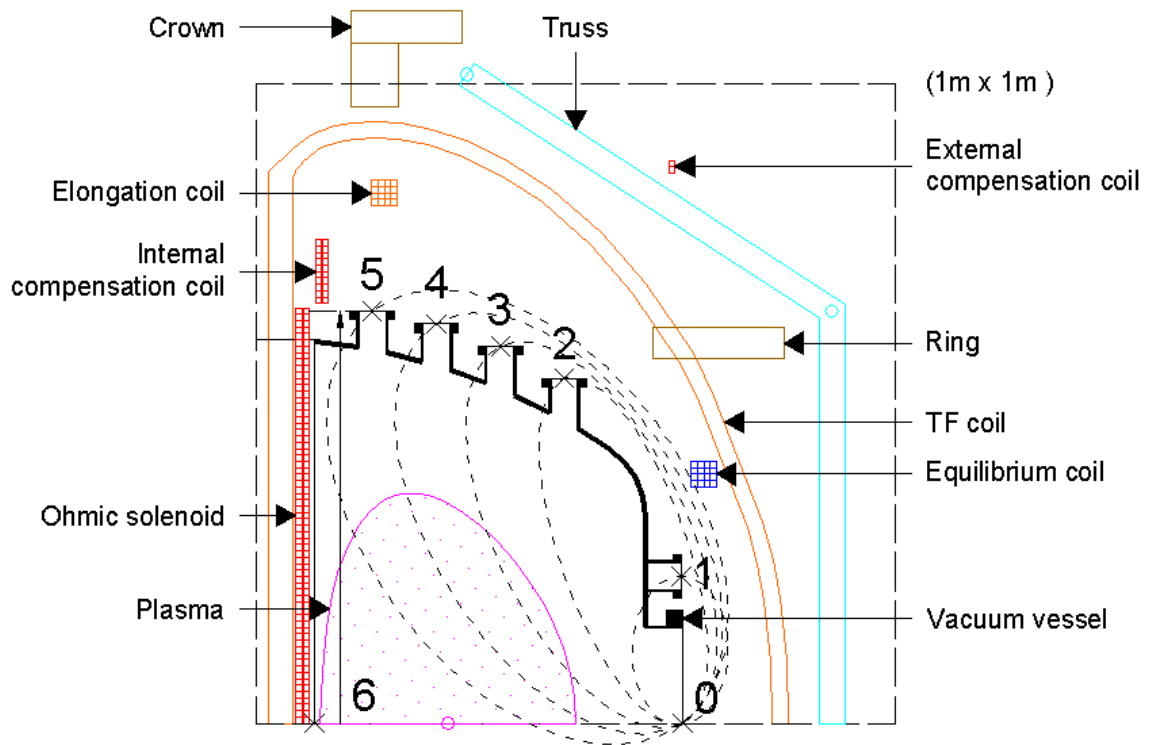Figure 4: *Distribution of eddy currents in sections of the ETE vacuum vessel.*

Figure 5: *Sections of the vacuum vessel used for measuring the eddy current distribution.*